J. J. Cuomo for Au film preparation, and P. A. Roland for carrying out computations. Helpful discussions with Dr. B. S. Berry and Dr. D. R. Campbell are also acknowledged.

[1]P. G. Shewmon, *Diffusion in Solids* (McGraw-Hill, New York, 1963), p. 174.
[2]R. W. Balluffi, Phys. Status Solidi 42, 11 (1970).
[3]M. Wuttig and H. K. Birnbaum, Phys. Rev. 147, 495 (1966).
[4]C. Baker, M. Wuttig, and H. K. Birnbaum, Trans. Japan Inst. Metals Suppl. 9, 268 (1968).
[5]D. Turnbull and R. E. Hoffman, Acta Met. 2, 419 (1954).
[6]R. F. Canon and J. P. Stark, J. Appl. Phys. 40, 436 (1969).
[7]W. R. Upthegrove and M. J. Sinnot, Trans. ASM 50, 1031 (1958).
[8]E. C. Oren and C. L. Bauer, Acta Met. 15, 773 (1967).
[9]T. E. Volin, K. H. Lie, and R. W. Balluffi, Acta Met. 19, 263 (1971).
[10]J. T. Robinson and N. L. Peterson, Surface Sci. 31, 586 (1972).
[11]A. Seeger and H. Mehrer, Phys. Status Solidi 29, 231 (1968).
[12]T. G. Stoebe and H. T. Dawson, Phys. Rev. 166, 621 (1968).
[13]W. Rupp, U. Ermert, and R. Sizmann, Phys. Status Solidi 33, 509 (1969).
[14]J. L. Whitton and G. V. Kidson, Can. J. Phys. 46, 2589 (1968).
[15]H. M. Morrison and V. L. S. Yuen, Can. J. Phys. 49, 2704 (1971).
[16]J. W. Matthews, Phil. Mag. 4, 1017 (1959).
[17]D. W. Pashley, Phil. Mag. 4, 324 (1959).
[18]D. Gupta and R. T. C. Tsui, Appl. Phys. Letters 17 294 (1970).
[19]D. Gupta (unpublished).
[20]Marz-grade Au was obtained from Materials Research Corp., Orangeburg, N. Y.
[21]The author is grateful to J. Angilello for carrying out Laue x-ray diffraction on Au films, and to C. F. Aliotta for examining the surfaces under electron microscope.
[22]Carrier-free Au^{195} was obtained from New England Nuclear, Boston, Mass.
[23]R. T. C. Tsui, Semicond. Proc. 10, 33 (1967).
[24]S. M. Makin, A. H. Rowe, and A. D. LeClaire, Proc. Phys. Soc. (London) 70, 545 (1957).
[25]J. C. Fisher, J. Appl. Phys. 23, 74 (1951).
[26]R. T. P. Whipple, Phil. Mag. 25, 1225 (1952).
[27]R. Smoluchowski, Phys. Rev. 87, 482 (1952).
[28]P. V. Pavlov *et al.*, Fiz. Tverd. Tela 6, 382 (1964) [Sov. Phys. Solid State 6, 305 (1964)].
[29]G. Brebec, Centre D'Etudes Nucleaires de Saclay Report No. CEA-R 2831, 1965 (unpublished).
[30]L. G. Harrison, Trans. Faraday Soc. 57, 1191 (1961).
[31]E. W. Hart, Acta Met. 5, 597 (1957).
[32]A. L. Ruoff and R. W. Balluffi, J. Appl. Phys. 34, 1848 (1963).
[33]C. T. Lai and H. M. Morrison, Can. J. Phys. 48, 1548 (1970).
[34]H. M. Morrison, Phil. Mag. 12, 985 (1965).
[35]R. N. Ghostagore, Phys. Rev. 155, 603 (1967).
[36]N. Q. Lam, S. J. Rothman, and L. J. Nowicki, Bull. Am. Phys. Soc. 17, 244 (1972).
[37]N. A. Gjostein, in *Techniques of Metals Research*, edited by R. A. Rapp (Interscience, New York, 1970), p. 447.
[38]M. Beyeler and Y. Adda, J. Phys. (Paris) 29, 345 (1968).

PHYSICAL REVIEW B VOLUME 7, NUMBER 2 15 JANUARY 1973

Anharmonicity in Noble Metals; Nonlinear Elasticity in Whiskers

Hiroshi Kobayashi* and Yosio Hiki
Tokyo Institute of Technology, Oh-okayama, Meguro-ku, Tokyo, Japan
(Received 6 March 1972)

A nonlinear stress-strain relation has been observed in copper whiskers with [100], [110], and [111] orientations using a sensitive apparatus for tensile-stress measurement. The nonlinearity was considered to be due to the lattice anharmonicity of the crystal. The nonlinearity constants of the specimens, which represent the amount of the deviation from linear elasticity, have been found to depend apparently on their yield stresses. Whiskers with low yield stresses showed large values of the nonlinearity constants. It was assumed that there was some kind of defects on the specimen surfaces and that the stress concentrations near the defects produced by the external forces lowered the yield stresses and increased the apparent nonlinearity constants. A simple analysis based on this assumption was enough to explain the experimental results, and the true nonlinearity constants which should be possessed by crystals without defects have been evaluated. The values of the true nonlinearity constants thus determined experimentally for three crystal orientations were consistent with the theoretical values from higher-order elasticity theory.

I. INTRODUCTION

The lattice vibrations of crystals are naturally anharmonic and some of the thermal, mechanical, and acoustic properties of solids are influenced markedly or are determined entirely by the lattice anharmonicity.[1-4] A continuum or elastic approximation can be adopted for treating the crystal an-

harmonicity when the dispersive nature of the lattice vibration is not essential. The finite-elasticity theory developed by Murnaghan[5] and the thermoelastic finite-deformation theory formulated by Thurston[6] and Wallace[3] are conveniently used in the treatment of anharmonicity. These theories predict that the stress-strain relations of solids deviate from linearity and the magnitudes of the deviation depend on the higher-order elastic constants, which are a measure of the anharmonicity of the crystals in the elastic approximation. It would be interesting if we could directly observe the nonlinear stress-strain relation of crystals, because not only could one then most directly ascertain the adaptability of the finite-elasticity theory to the real solids but one could also obtain the information about the higher-order elastic constants of the materials.

When typical single crystals of pure metals are deformed, plastic flow easily occurs before enough stress is applied for observing the elastic nonlinearity. The only possible way to observe elastic nonlinearity may be to use whisker crystals, as Seeger and Buck suggested,[7] because whiskers have an extremely high yield strength, possibly owing to the structural perfection.[8–10] Although nonlinear behavior has sometimes been observed in tensile stress-strain tests of metallic and nonmetallic whiskers,[11–14] it was not related to the nonlinear elasticity of the materials. Powell and Skove[15] first attempted to measure the elastic nonlinearity in copper, silver, and iron whiskers for the purpose of determining the third-order elastic constants. They used a rather indirect method to determine the nonlinearity, applying a low-frequency, uniaxial, oscillatory force superposed upon the steady tensile force. Their results on the magnitude of the nonlinearity were, however, scattered from specimen to specimen beyond the experimental error. More direct experiments on the elastic behavior of whiskers is desirable.

The present investigation was aimed to directly observe the nonlinear stress-strain relations of noble-metal whiskers using a sensitive tensile-stress apparatus, and to compare the results with the predictions of higher-order elasticity theory. Gold whiskers were excluded because specimens long enough for the tensile experiment were difficult to grow. Difficulties were also experienced in the case of silver whiskers, as straight specimens with uniform diameters could be grown very rarely. Only the results on copper whiskers with [100], [110], and [111] axial orientations will be described in the present paper.

II. EXPERIMENTAL PROCEDURE

A. Apparatus

A sensitive apparatus should be used for the present purpose to record the stress-strain curves of whiskers in their elastic region. For example, for metal whiskers having yield stresses of the order of 100 kg/mm^2, of a few μ in diameter and 1 mm in length, the maximum load and elongation in the tensile experiment is around a few g and 10^{-3} cm, respectively. The tensile apparatus adopted is a variant of an analytical balance with the specimen attached to one arm and a solenoid-magnet system to the other arm for loading the specimen. Each end of the specimen is glued to the upper mounting rod suspended from the arm and to the lower fixed mounting rod. The loading system can apply forces ranging from a few mg to a few g by changing the current in the solenoid. Slow and smooth loading is realized by driving the moving edge of a variable resistor in the current-supply circuit using a motor and gear box. The voltage across a standard resistor in the circuit is fed to the Y axis of an X-Y recorder. As the specimen is elongated, a mirror attached to the end of the balance arm is rotated. The amount of the rotation is detected with an optical lever which converts the rotation into a change of output voltage electro-optically. This voltage is fed to the X axis of the recorder after being amplified by a DC amplifier. The load-elongation curve of the specimen is traced automatically. A slow elongation rate of 10^{-5}– 10^{-6}/sec was always used in the present experiment.

The design of the optical lever is essentially the same as that described by Jones and Richards.[16] Using a lamp and lens system, the image of a glass grating is superposed onto a second grating after reflection by the rotating mirror. When the mirror is rotated, the image on the grating is moved in the direction perpendicular to the bars of the gratings. The first grating is composed of dark and transparent bars with equal widths, while the second grating is the same as the first except that it is divided by a central dark bar which is just twice the width of the usual ones. When the right half of the second grating passes light from the first grating, the left half stops the light. The situation is reversed when the mirror is rotated by some amount and the image of the first grating is shifted just one bar length. The right and left halves of the light beam are separated after passing through the second grating, and each is projected upon a photomultiplier. The photocurrents in the two photomultipliers increase and decrease exactly out of phase as the mirror is rotated. The difference between the currents is proportional to the rotation angle of the mirror and therefore to the specimen elongation. Using gratings with 20 dark bars per cm, the maximum measurable value of the specimen elongation is about 70 μ in the present case.

The reliability of the load measurement is a few

mg, which is mostly determined by the sensitivity of the balance. Thermal disturbances of the air in the light beams of the optical system are the main limit to the reliability of the elongation measurement, which is estimated to be about 0.05μ under typical conditions. A full description of the apparatus appears in a separate paper.[17]

B. Specimen Preparation and Manipulation

Copper-whisker specimens were grown using the reduction method developed by Brenner.[18] Satisfactory result was obtained by hydrogen reduction of a 1:1 mixture of CuI and CuBr at 600 °C. The reaction time was 2–3 h and the flow rate of hydrogen was about 100 cm^3/min. The lengths and diameters of the grown whiskers were 0.2–5 cm and 1–20 μ, respectively. Both chemical and atomic-absorption spectroscopy of the specimen material showed that the impurities contained were 0.020-at.% Fe and 0.0005-at.% Ag. Whiskers of a few mm in length and about 3–4 μ in diameter with straight and uniform shapes and with good surface condition were chosen for the tensile experiments after inspection with a microscope.

Extreme care was taken to manipulate the specimen whiskers, because improper handling easily caused plastic deformation and produced surface slip traces. A refined technique using a special manipulator was adopted to set the specimen in the testing position.[17] The specimen was glued to the upper mounting rod with diphenyl carbazide, and to the lower rod with aron-alpha (alpha-cyanoacrylate). After mounting the specimen, the gage length was measured with a telescope. The diameter of the specimen was determined after the tensile test had been done. The portion of the specimen within the adhesive agent was cut with a razor blade, and the cross-sectional area was measured from photomicrographs (×1500–×3000). The square root of the measured area was employed as the "diameter" of the specimen. The crystal orientations of the whiskers were determined by the rotating-crystal x-ray method. Almost all whiskers had [100], [110], or [111] axial orientations.

III. RESULTS AND ANALYSIS

A. Experimental Results

A typical example of recorded stress-strain curves of whiskers with different orientations is shown in Fig. 1, where P is the apparent stress defined as the applied load divided by the cross-sectional area of the undeformed specimen, and ϵ is the usual strain equal to the specimen elongation divided by the gage length. Deviations from linear relationship between stress and strain can be seen in these curves. The dashed lines are those having slopes with the apparent Young's moduli of the specimens. These stress-strain curves were used to analyze the nonlinear elasticity of the specimens. In the typical experiment the load was increased until the specimen yielded and fractured. When the load was decreased before yielding, very slight differences were sometimes seen in the increasing-load and decreasing-load curves ([110] specimen), which might be due to the mechanical hysteresis of the apparatus. It seemed, however, that no permanent strain remained after the load was diminished, and the deformation of the specimen was considered to be elastic. The anomaly sometimes observed at low stress level ([111] specimen) might be due to the misalignment of the specimen setting and this part of the curve was omitted in the analysis.

The nonlinearity between strain and stress is conveniently expressed as follows[7]:

$$\epsilon = P/E + \delta(P/E)^2 . \tag{1}$$

In the limit of infinitesimal deformation, stress is proportional to strain and their ratio E is the apparent Young's modulus. The quantity δ is called the nonlinearity constant, which represents the nonlinear elasticity of the specimen. In Fig. 2, as an example, ϵ/P is plotted against P using the stress-strain data of Fig. 1, and reasonably linear relationships hold between the two quantities. Experimental values of Young's modulus E_{expt} and nonlinearity constant δ_{expt} can be determined from least-squares fits to the data. The values for various specimens are compiled in Table I, together with the diameter and gage length of the specimens. The maximum stress where yield of the specimen occurs, P_{max}, is also indicated in the table. The reliability of the measured values of Young's modulus and nonlinearity constant is mostly limited by the accuracy of the specimen

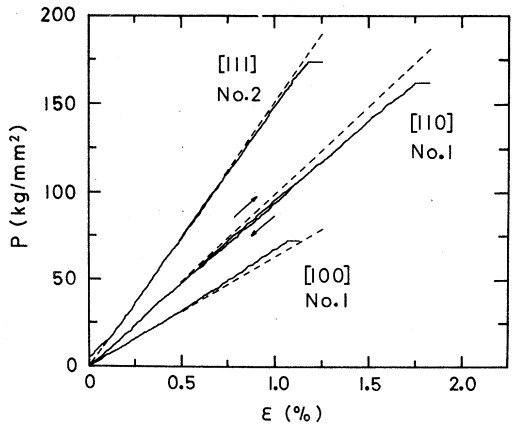

FIG. 1. Typical stress P vs strain ϵ curves of copper whiskers with different orientations.

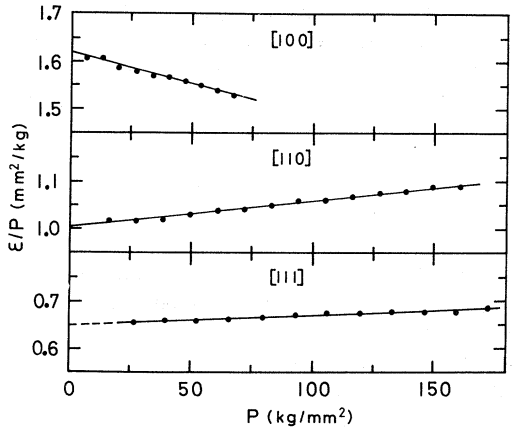

FIG. 2. Plots of ϵ/P against P for the stress-strain relations of Fig. 1.

diameter measurement, which is around 10% or better in typical cases.

B. Nonlinear Elasticity

The nonlinearity constant δ appearing in the stress-strain relation of Eq. (1) can be calculated theoretically using higher-order elasticity theory. In finite deformation of materials, the Lagrangian strain tensor η_{ij}, defined as

$$\eta_{ij}=\frac{1}{2}\left(\frac{\partial x_k}{\partial a_i}\frac{\partial x_k}{\partial a_j}-\delta_{ij}\right)$$

$$=\frac{1}{2}\left(\frac{\partial u_i}{\partial a_j}+\frac{\partial u_j}{\partial a_i}+\frac{\partial u_k}{\partial a_i}\frac{\partial u_k}{\partial a_j}\right), \tag{2}$$

is conveniently used to represent the deformed state, where a_i and x_i are the coordinates of a material point before and after the deformation and $u_i=x_i-a_i$ is the displacement. Summation over repeated indices is always implied. The stress component σ_{ij} is defined as the force applied per unit area of the deformed material, and the Lagrangian strain derivative of the energy density of the material is not equal to the stress when the deformation is finite because the strain is defined referred to the coordinates of the undeformed state. It is more profitable to use the thermodynamic tension t_{ij} defined as

$$dW=t_{ij}d\eta_{ij}, \tag{3}$$

where dW is the work done per unit volume of undeformed material. The relation

$$t_{ij}=\left(\frac{\partial(\rho_0 F)}{\partial\eta_{ij}}\right)_T=\left(\frac{\partial(\rho_0 U)}{\partial\eta_{ij}}\right)_S \tag{4}$$

then follows directly from the definition, where F and U are the Helmholtz free energy and the internal energy of unit mass of material, respectively, ρ_0 is its density before deformation, and T and S indicate, respectively, the isothermal and adiabatic conditions. The isothermal and adiabatic elastic stiffness constants of nth order are defined as

$$C^T_{ijklmn\cdots}=\rho_0\left(\frac{\partial^n F}{\partial\eta_{ij}\partial\eta_{kl}\partial\eta_{mn}\cdots}\right)_T,$$

$$C^S_{ijklmn\cdots}=\rho_0\left(\frac{\partial^n U}{\partial\eta_{ij}\partial\eta_{kl}\partial\eta_{mn}\cdots}\right)_S. \tag{5}$$

The free energy and the internal energy of strained material are each expanded as a power series of strain, with the elastic constants as coefficients:

$$\rho_0 F(\eta_{ij},T)=\rho_0 F(0,T)+\frac{1}{2!}c^T_{ijkl}\eta_{ij}\eta_{kl}+\frac{1}{3!}C^T_{ijklmn}\eta_{ij}\eta_{kl}\eta_{mn}+\cdots,$$

$$\rho_0 U(\eta_{ij},S)=\rho_0 U(0,S)+\frac{1}{2!}c^S_{ijkl}\eta_{ij}\eta_{kl}+\frac{1}{3!}C^S_{ijklmn}\eta_{ij}\eta_{kl}\eta_{mn}+\cdots. \tag{6}$$

It can be shown, through a thermodynamic argument, that the relation between the usual stress σ_{kl} and the thermodynamic tension t_{ij} is[6]

$$t_{ij}=J\sigma_{kl}\frac{\partial a_i}{\partial x_k}\frac{\partial a_j}{\partial x_l}, \tag{7}$$

where J is the Jacobian determinant

$$J=\left|\frac{\partial(x_1,x_2,x_3)}{\partial(a_1,a_2,a_3)}\right|. \tag{8}$$

The nonlinear force-deformation relation can be derived from Eq. (7) when the material is strained with special mode of deformation. In such a case, the x_i's are expressed with a_i's, and the right-hand side of the equation can be represented as a function of u_i, a_i and the applied force. On the other hand, t_{ij} is related to η_{ij} and $C_{ijkl}\cdots$ using Eqs. (4) and (6), while η_{ij} can be expressed using u_i and a_i, as Eq. (2) shows.

In the case of a long specimen with uniform

TABLE I. Summary of experimental results.

Specimen	Number	Diameter (μ)	Length (mm)	δ_{expt}	E_{expt} 10^4 (kg/mm²)	P_{max} (kg/mm²)
[100]	1	4.9	0.95	−6.5	0.616	71
	2	4.7	1.07	−2.2	0.667	143
	3	4.0	1.10	−14.2	0.565	38
	4	4.5	1.20	−8.2	0.393	65
	5	3.6	0.97	−4.5	0.598	177
[110]	1	3.4	0.84	9.2	0.991	162
	2	2.8	0.72	12.7	0.936	91
	3	3.3	0.58	18.0	1.036	60
[111]	1	3.2	1.35	10.2	1.442	102
	2	3.2	1.25	4.7	1.508	174
	3	3.9	1.20	10.1	1.257	104
	4	2.5	0.97	4.5	1.372	162

cross section deformed homogeneously along its axis, the nonlinear stress-strain relation is easily expressed in the form of Eq. (1), and the nonlinearity constant δ can be represented as a function of second- and third-order elastic constants. For a specimen with axis of [100] direction, Young's modulus E and the nonlinearity constant δ are

$$E = c_{11} - 2c_{12}\nu, \quad \nu = c_{12}/(c_{11}+c_{12}) ,$$

$$\delta = -\frac{3}{2} + \frac{1}{c_{11}(c_{11}+c_{12}) - 2c_{12}^2}\{\tfrac{1}{2}[2c_{12}\nu^2 - (c_{11}+c_{12})]C_{111} + [(2c_{12}-c_{11})\nu^2 + 2c_{11}\nu + c_{12}]C_{112} - [(c_{11}+c_{12})\nu^2 + 2c_{12}\nu]C_{123}\} . \quad (9)$$

Similar expressions are also obtained for the [110] and [111] directions, and they are the same as those described by Seeger and Buck,[7] except that the thermodynamically-defined elastic constants[19] [Eq. (5)] are used in the present case instead of Birch's constants.[20] The nonlinearity constant δ for the [100] direction contains a linear combination of three third-order elastic constants C_{111}, C_{112}, and C_{123}, while that for the [110] direction includes five constants C_{111}, C_{112}, C_{123}, C_{144}, and C_{166}, and that for the [111] direction includes all six constants.

The nonlinearity constant δ can be calculated using the experimental values of third-order elastic constants. It must be noticed that the observation of the nonlinear stress-strain relations is usually done under isothermal conditions and the isothermal elastic constants should be used for the calculation. Third-order elastic constants are usually determined by acoustic measurements, and the values obtained are of mixed type,

$$C^M_{ijklmn} = \rho_0\left(\frac{\partial(\partial^2 U/\partial\eta_{ij}\partial\eta_{kl})_S}{\partial\eta_{mn}}\right)_T , \quad (10)$$

because they are derived from the dependence of ultrasonic velocity on hydrostatic and uniaxial stress.[6,21] The isothermal third-order elastic constants can be derived from the mixed constants through the following relations[22]:

$$C^T_{ijklmn} - C^M_{ijklmn} \simeq -T(\rho_0\gamma C_t)^{-1} \times [\alpha_{rs}\alpha_{pq}(c^S_{ijrs}C^M_{klpqmn} + c^S_{klpq}C^M_{ijrsmn}) + c^S_{ijrs}c^S_{klpq}(\alpha_{rs}\beta_{pqmn} + \alpha_{pq}\beta_{rsmn})] , \quad (11)$$

$$\gamma = C_t/C_\eta = 1 + Tc^S_{ijkl}\alpha_{ij}\alpha_{kl}(\rho_0 C_t)^{-1} ,$$

$$\beta_{pqmn} \simeq \left(\frac{\partial\alpha_{pq}}{\partial\eta_{mn}}\right)_T = c^T_{tumn}\left(\frac{\partial s^T_{pqtu}}{\partial T}\right)_t ,$$

where C_t and C_η are the specific heat under the condition of constant thermodynamic tension or constant strain, α_{ij} is the thermal-expansion coefficient, and s_{pqtu} is the elastic compliance constant. The relation between the isothermal and adiabatic second-order elastic constants is also to be noted:

$$c^T_{ijkl} - c^S_{ijkl} = -T\alpha_{rs}\alpha_{pq}c^S_{ijrs}c^S_{klpq}(\rho_0\gamma C_t)^{-1} . \quad (12)$$

The adiabatic second-order constants are directly determined from sound velocity measurements.

The values of Young's modulus E and the nonlinearity constant δ were calculated for three different specimen orientations using the second-[23] and third-order[23,24] elastic constants of copper. The results are shown in Table II, where δ_{I} and δ_{II} represent the values obtained by using the third-order constants due to Hiki and Granato, and Salama and Alers, respectively. The adopted values of the temperature derivatives of elastic compliance, which are required to convert the mixed elastic constants into isothermal ones, are those measured by Overton and Gaffney.[25]

TABLE II. Calculated values of Young's modulus and nonlinearity constant.

Direction	E (10^4 kg/mm^2)	δ_{I}	δ_{II}
[100]	0.678	−4.51	−2.00
[110]	1.325	10.57	7.23
[111]	1.941	3.76	2.68

C. Interpretation of Results

It is seen from Table I that even for specimens of the same orientation, the experimental values of nonlinearity constant δ_{expt} and Young's modulus E_{expt} vary greatly from specimen to specimen. These quantities represent the second- and third-order elasticity of crystals and should not be originally so structure sensitive. The measured values of Young's modulus of the whiskers were always smaller than the values calculated from the elastic constants of bulk crystals, and this tendency has also been reported by other authors.[14] In the present experiment, the lowering of the apparent Young's modulus is considered to be due to the deformation of the adhesive agent used to glue the specimen. The aim of the present experiment is to measure the nonlinearity constant, so that the inaccuracy in Young's modulus measurement is disregarded. The measured values of the nonlinearity constant are widely spread among specimens with the same orientation, and the situation is the same as the data by Powell and Skove.[15] They assumed that the third-order elastic constants were sensitive to the impurity concentration, and that the variation of the values of nonlinearity constant was due to the scatter of

the purities of whiskers used. However, the third-order constants of noble metals may not be much influenced by impurities, because the values are mainly determined by the closed-shell repulsive forces between the ion cores in the crystal owing to the large d-shell overlaps.[23] It is also difficult to assume that the purities of whiskers vary much from specimen to specimen when they are grown under the same condition from the same materials.

Although at first sight the nonlinearity values seem to scatter at random, it was found that considerable regularity exists when the values of δ_{expt} were plotted against P_{max}, the maximum stress where the yield of the specimen occurred. These plots are shown in Fig. 3, and it can be seen that specimens with low yield stresses have noticeably higher values of the nonlinearity constant. It is tentatively assumed that for specimens with low yield stresses there is some kind of "defect" in the specimen, or on the surfaces of the specimen, which lowers the yield stress and also increases the apparent value of the nonlinearity constant. The defects may produce concentration of stresses when the external force is applied to the specimen and yield occurs at low levels of external stress, while the apparently large nonlinearity constant may be observed because the real stress in the specimen is higher than that predicted from the external force. A simple argument and an analysis of the experimental data will be presented with this idea.

When a force is applied to a whisker crystal, the total stress P in the specimen is assumed to be

$$P = P_e + P_i \,, \tag{13}$$

where P_e is the externally applied stress which is uniform throughout the specimen, and P_i is the internal stress caused from the concentration of stress near the defects. As the external stress is increased the internal stress also increases,

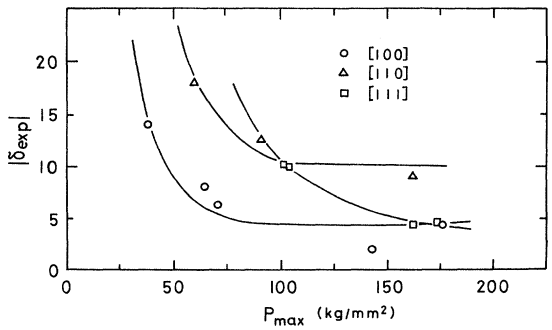

FIG. 3. Experimental nonlinearity constants δ_{expt} plotted against yield stresses P_{max} for three specimen orientations.

and its amount depends on the position in the specimen. Because the diameters of the whisker specimens are extremely small compared with their lengths, the variation of the internal stress along the radial direction of the specimen may be neglected compared with that along the specimen axis. It is assumed that the internal stress varies with position in the specimen as

$$P_i = P_e k \sin 2\pi x/\lambda \,, \tag{14}$$

where x is the distance along specimen axis, λ is the "wavelength" of the stress, and k is a constant. This assumption means that the varying internal stress is approximated by the first term of its Fourier components, and λ has the meaning of the average spacing between the defects. By inserting Eqs. (13) and (14) into Eq. (1), we obtain

$$\epsilon(x) = (P_e/E)(1 + k \sin 2\pi x/\lambda) + \delta(P_e/E)^2 (1 + 2k \sin 2\pi x/\lambda + k^2 \sin^2 2\pi x/\lambda) \,.$$

After averaging the strain along the specimen length, one obtains

$$\epsilon = P_e/E + \delta(P_e/E)^2 (1 + \tfrac{1}{2} k^2) \tag{15}$$

as the relation between the external stress and the strain of the specimen. Thus, the experimentally obtained value of the nonlinearity constant can be expressed as

$$\delta_{expt} = \delta(1 + \tfrac{1}{2} k^2) \,, \tag{16}$$

where δ is the true value of the constant of the material. On the other hand, the specimen is assumed to yield when the total stress P is increased to an "ideal" yield stress P_0 which is a quantity proper to the material and the specimen orientation. From Eqs. (13) and (14),

$$P_0 = P_{max} + k P_{max} \,, \tag{17}$$

and P_{max} is the observed value of the yield stress of the specimen. By eliminating the constant k from Eqs. (16) and (17), one arrives at the relation

$$\delta_{expt} = \tfrac{1}{2}[(P_0/P_{max})^2 - 2(P_0/P_{max}) + 3]\delta \,. \tag{18}$$

The most probable values of the true nonlinearity constant δ and the ideal yield stress P_0 of the crystals can be evaluated using the sets of values of P_{max} and δ_{expt} measured for several specimens of the same orientation.

A computer calculation was carried out to obtain the values of δ and P_0 for each orientation of the crystal. By choosing a value of P_0, the constant δ is determined for each specimen from Eq. (18) with the experimental values of δ_{expt} and P_{max}. The sum of the square of $\Delta = \delta - \delta_{expt}$ for all specimens with the same orientation, $\Sigma\Delta^2$, is computed. A set of values of δ and P_0 for which $\Sigma\Delta^2$ has minimum value is chosen as being most probable. An

example of how the values of δ and $\Sigma\Delta^2$ vary with P_0 can be seen in Fig. 4. The most probable values of δ and P_0 obtained are tabulated in Table III for three crystal orientations. The probable errors in δ's are reduced from the corresponding $\Sigma\Delta^2$ values. By using these δ and P_0 values together with Eq. (18), the values of δ_{expt} are recalculated as a function of P_{max}; and the curves in Fig. 3 show the results. In spite of the simplifying assumptions adopted, the variation of δ_{expt} with P_{max} seems to be rather well represented by the relation of Eq. (18). It is also seen that the computed values of δ are close to the theoretical nonlinearity constant δ_I in Table II.

IV. DISCUSSION

The nonlinearity observed in the stress-strain relation of whiskers is considered to really originate from the anharmonicity of the crystal. The possibilities of deviation from linearity arising from instrumental origins were ruled out after careful checks of the apparatus. If crystal dislocations were present in the specimen, they could move and produce extra strain when stress is applied. Such dislocation movement will, however, usually produce permanent strain when the stress is diminished. No such permanent strain was observed in the present case. Furthermore, direct observations by x-ray diffraction topography[26,27] and electron microscopy[28] show that in almost all cases there is no dislocation in copper whiskers produced by hydrogen reduction. The nonlinearity constants determined from the stress-strain curves were at first sight incredibly scattered from specimen to specimen. A systematic relation was found to exist between the measured nonlinearity constants and the observed yield

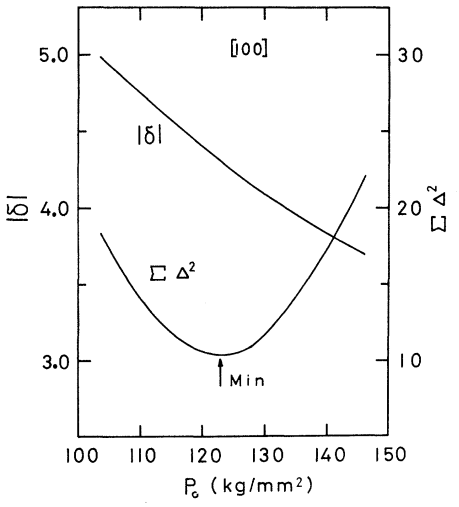

FIG. 4. Procedure for determining the most probable values of δ and P_0.

TABLE III. True nonlinearity constants and ideal yield stresses derived from experiments.

Direction	δ	P_0 (kg/mm^2)
[100]	-4.3 ± 0.5	123
[110]	10.0 ± 0.5	138
[111]	3.5 ± 0.1	306

stress of the specimens, and analysis was made on the basis of a simple model to explain the relation. The explanation seems to be consistent, but further discussion should be given concerning the adopted model and the results of the analysis.

Some kind of "defects" which lower the yield stresses and increase the apparent nonlinearity constants were assumed to exist in whisker crystals. The nature of the defects is such as to produce extra stress only when a force is applied to the specimen. Dislocations and point defects which have permanent stress fields around themselves are excluded. Surface defects such as growth steps, which can often be observed in metal whiskers, [10] are most likely the defects assumed in the present case. Brenner[29] found that the smaller the specimen diameters of metal whiskers, the higher their yield stresses. This fact is usually explained through an argument such that the yield stresses of whiskers are mainly determined by surface defects because the abundance of the defects is proportional to the surface area of the specimens. The stress concentration around the defects is considered to induce the generation of dislocations, and once dislocations are generated they can propagate throughout the crystal and yielding occurs. Transmission electron microscopy[30,31] and x-ray topography[32] also show that the first traces of plastic deformation start near the surface defects or surface irregularities. In the present experiment, it might be desirable to show the existence of defects on the surfaces of whiskers which have low yield stress and high nonlinearity constant values. These trials were abandoned because of technical difficulties.

In the present analysis, it is assumed that yielding occurs when the sum of the external stress and the stress caused from the defects is increased up to the "ideal" yield stress P_0 somewhere in the specimen. The stress P_0 is interpreted as the stress enough to generate crystal dislocations. The values of the "ideal" yield strain, P_0/E, are 0.018, 0.010, and 0.016 for [100], [110], and [111] whiskers. The theoretical maximum strain to destroy the perfect crystal can be evaluated as $\frac{1}{6}-\frac{1}{30}$ through a simple argument.[33] The P_0/E values are smaller than these values, which suggest that dislocations can be produced before the stresses reach the values sufficient for breaking

the bonds between atoms in the crystal. The generation of dislocations may be a statistical process, and the ideal yield stress P_0 determined for a set of several specimens has only the meaning of the average stress for the generating process. It is thus not unreasonable that some of the specimens have yield stresses P_{max} larger than P_0 (in the case of [100] and [110]). Finally, it is noticed that the computed values of the "true" nonlinearity constant δ, which are considered to be those of crystals without defect, are not inconsistent with the theoretical values from higher-order elasticity theory. The apparent agreement between the values of δ and the theoretical values δ_I calculated by using the third-order elastic constants determined by Hiki and Granato, however, should not be so strongly emphasized, because several assumptions are adopted in the course of the analysis of the data, and also because it seems that in the present experiment there are not enough data on specimens with high yield stress.

In conclusion, the direct measurement of nonlinearity in the elasticity of whiskers is possible, and the accurate measurement may be carried out for determining the third-order elastic constants, or at least their combinations, when enough care is taken with regard to the fact that specimens with low yield stress are not adequate for that purpose.

ACKNOWLEDGMENTS

We would like to thank T. Ishihama, T. Singyoji, and T. Nawa for their help with the experiments, and Y. Kogure for his assistance in processing the data.

*Present address: National Research Laboratory of Metrology, Itabashi-ku, Tokyo.

[1]G. Leibfried and W. Ludwig, Solid State Phys. **12,** 275 (1961).
[2]P. G. Klemens, Solid State Phys. **7,** 1 (1958).
[3]D. C. Wallace, Solid State Phys. **25,** 301 (1970).
[4]R. Truell, C. Elbaum, and B. B. Chick, *Ultrasonic Methods in Solid State Physics* (Academic, New York, 1969).
[5]F. C. Murnaghan, *Finite Deformation of an Elastic Solid* (Wiley, New York, 1951).
[6]R. N. Thurston, Phys. Acoust. IA, 1 (1964).
[7]A. Seeger and O. Buck, Z. Naturforsch. **15a**, 1056 (1960).
[8]*Growth and Perfection of Crystals*, edited by R. H. Doremus *et al.* (Wiley, New York, 1958).
[9]É. M. Nadgornyĭ, Yu. A. Osip'yan, M. D. Perkas, and V. M. Rozenberg, Usp. Fiz. Nauk **67,** 625 (1959) [Sov. Phys.-Usp. **67,** 282 (1959)].
[10]É. M. Nadgornyĭ, Usp. Fiz. Nauk **11,** 201 (1962) [Sov. Phys.-Usp. **5,** 462 (1962)].
[11]S. S. Brenner, Ref. 8, p. 157.
[12]N. Cabrera and P. B. Price, Ref. 8, p. 204.
[13]J. E. Gordon, Ref. 8, p. 219.
[14]K. Yoshida, Y. Gotoh, and M. Yamamoto, J. Phys. Soc. Jap. **24,** 1099 (1968).
[15]B. E. Powell and M. J. Skove, Phys. Rev. **174,** 977 (1968).
[16]R. V. Jones and J. C. S. Richards, J. Sci. Instrum. **36,** 90 (1959).
[17]H. Kobayashi and Y. Hiki, Jap. J. Appl. Phys. **11,** 738 (1972).
[18]S. S. Brenner, Acta Metall. **4,** 62 (1956).
[19]K. Brugger, Phys. Rev. 133, A1611 (1964).
[20]F. Birch, Phys. Rev. **71,** 809 (1947).
[21]R. N. Thurston and K. Brugger, Phys. Rev. 133, A1604 (1964).
[22]B. E. Powell and M. J. Skove, J. Appl. Phys. **38,** 404 (1967).
[23]Y. Hiki and A. V. Granato, Phys. Rev. **144,** 411 (1966).
[24]K. Salama and G. A. Alers, Phys. Rev. **161,** 673 (1967).
[25]W. C. Overton, Jr. and J. Gaffney, Phys. Rev. **98,** 969 (1955).
[26]V. G. Lyuttsau, Yu. M. Fishman, and I. L. Svetlov, Sov. Phys.-Crystallogr. **10,** 707 (1966).
[27]O. Nittono and S. Nagakura, Jap. J. Appl. Phys. **8,** 1180 (1969).
[28]M. Yamamoto, Y. Gotoh, K. Yoshida and D. Watanabe, J. Crysl. Growth **3/4,** 705 (1968).
[29]S. S. Brenner, J. Appl. Phys. **27,** 1484 (1956).
[30]P. B. Price, Philos. Mag. **5,** 873 (1960).
[31]P. B. Price, Proc. R. Soc. **A268,** 251 (1961).
[32]O. Nittoni, Jap. J. Appl. Phys. **10,** 188 (1971).
[33]A. H. Cottrell, *Dislocations and Plastic Flow in Crystals* (Clarendon, Oxford, England, 1953), p. 8.